Influence of envelope, structural thermal mass and indoor content on the building heating energy flexibility

Johra, Hicham; Heiselberg, Per Kvols; Le Dréau, Jérôme

Published in:
Energy and Buildings

DOI (link to publication from Publisher):
10.1016/j.enbuild.2018.11.012

Publication date:
2019

Document Version
Accepted author manuscript, peer reviewed version

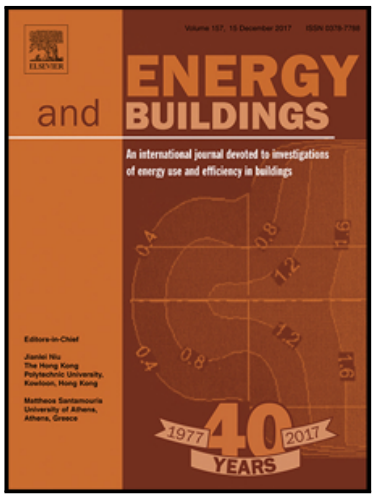

Influence of envelope, structural thermal mass and indoor content on the building heating energy flexibility

Hicham Johra , Per Heiselberg , Jérôme Le Dréau

PII: S0378-7788(17)33856-2
DOI: https://doi.org/10.1016/j.enbuild.2018.11.012
Reference: ENB 8887

To appear in: *Energy & Buildings*

Received date: 28 November 2017
Revised date: 11 June 2018
Accepted date: 12 November 2018

Please cite this article as: Hicham Johra , Per Heiselberg , Jérôme Le Dréau , Influence of envelope, structural thermal mass and indoor content on the building heating energy flexibility, *Energy & Buildings* (2018), doi: https://doi.org/10.1016/j.enbuild.2018.11.012

Highlights

- Influence of building characteristics on heating energy flexibility of dwellings.
- Envelope insulation level is the dominant parameter, followed by thermal inertia.
- PCM systems can appreciably improve energy flexibility of light-structure houses.
- Indoor items / furniture should be included in light-structure building models.

Energy and Buildings

Influence of envelope, structural thermal mass and indoor content on the building heating energy flexibility

Hicham Johra [a, *], Per Heiselberg [a], Jérôme Le Dréau [b]

[a] *Aalborg University, Division of Architectural Engineering, Department of Civil Engineering, Thomas Manns Vej 23, DK-9220 Aalborg Øst, Denmark*

[b] *LaSIE UMR CNRS 7356, La Rochelle University, FR-17 000 La Rochelle, France*

** Corresponding author. Tel.: +45 9940 7234. E-mail address: hj@civil.aau.dk (H. Johra).*

Abstract

This article presents the results of a numerical study investigating the influence of the main building parameters on the indoor space heating energy flexibility of a Danish house. The focus is placed here on the envelope insulation level, the structural thermal mass, the additional thermal mass of indoor content (indoor items/furniture, PCM integrated in furnishing, PCM wallboards) and the type of heating system. The heating energy flexibility is defined as the dwelling's ability to shift heating use in time without jeopardizing indoor comfort and technical constraints. A heat storage strategy with indoor temperature set point modulation controlled by a price signal is implemented in the building model. It is shown that the insulation level of the envelope is the building's characteristic with the largest effect on the heating energy flexibility. To a lesser extent, the total thermal inertia also presents a significant influence. It was also found that the presence of indoor items and furniture in the built environment can increase the building time constant and energy flexibility potential by up to 42% and 21% respectively, in the case of dwellings with low structural thermal mass. Finally, phase change materials integrated in wallboards or in furnishing elements can increase substantially the time constant and heating energy flexibility of a house.

Keywords: Building energy flexibility; demand-side management; indoor space heating; indoor thermal mass; enveloppe thermal inertia; phase change material; furniture.

1. Introduction

Most of the current national energy development strategies involve a large expansion of renewable energy sources (RES). A significant deployment of wind and photovoltaic power is planned in numerous European countries [1]. In Denmark, for example, the share of wind power is expected to reach 50% on an annual basis in 2020. In 2050, Denmark aims at covering its entire energy needs with RES [2].

The major drawback of RES is that their production is intermittent and difficult to modulate. The important expansion of these intermittent RES may thus induce a serious mismatch between instantaneous energy use and production. Consequently, the stability of electrical grids can be significantly compromised. In the recent years, increasing efforts have been dedicated to develop demand-side management technologies allowing a modulation of the end-users' energy need and consumption. These so-called "energy flexible" solutions can counter-balance the irregularities of RES production in an integrated Smart Grid system. It improves the controllability of the energy grids and therefore eases the integration of RES [3].

In many countries, buildings hold the largest share of the total energy needs. Moreover, 75% of the buildings energy use in Europe is dedicated to indoor space heating [4]. To a certain extent, the energy used for the conditioning of the built environment can be shifted in time without jeopardizing indoor comfort. To that matter, the thermal heat capacity of the buildings' envelope and structural elements can present large potential for energy storage. Therefore the building sector should not be perceived as a passive energy end-user. On the contrary, it can be an important interactive actor, modulating its energy utilisation to facilitate the management of energy grids. The passive thermal energy storage

(TES) in the indoor environment of buildings can be a cost effective key component for the management strategies of a smart energy grid system. A research study indicated that this clever usage of the building thermal inertia allows a larger reduction of excess electricity production and fuel consumption with a lower total cost compared to the heat accumulation water tanks solution [5]. The building set point indoor temperature can be increased to accumulate heat when the electricity is available and cheap and can be decreased when the power production is too low. However, the operative temperature should always be kept within the limits of the occupants' thermal comfort.

Some previous studies investigated the influence of different building parameters on the ability to modulate heating needs. In the case of TES in the indoor environment, the available thermal mass defines the maximum storage capacity of the system. The larger the thermal mass, the more heat energy can be stored during off-peak periods and partly recovered during peak periods [6] [7].

The effectiveness of the indoor space thermal storage mainly depends on the envelope performance: level of insulation and air tightness. With a higher envelope performance, a building can conserve thermal energy over a larger period of time which contributes to the temporal aspect of its energy flexibility [6] [8]. Poorly insulated buildings can only sustain short term load shifting. In winter, after a heat accumulation period, they can maintain thermal comfort without any heating need for a maximum of 1 – 5 hours whereas high performance envelope buildings can turn off their heaters for more than 24 hours. Consequently, a large amount of thermal energy can be shifted over a short period of time for low-insulation buildings while the well-insulated ones can shift a smaller quantity of energy over a long period of time [9].

Moreover, it was found that the type of heat emitter has a significant influence on the heating energy flexibility. On the one hand, radiator terminals have mainly convective heat emission which results in a quick activation of the low capacitive indoor air. Therefore, the ventilation and infiltration heat losses are increased and the heat storage in the structural heavy building elements is limited. On the other hand, radiant emitters such as under-floor heating (UFH) or thermally activated building systems (TABS) can activate directly the high thermal capacity of the floor elements. The time constant of the building increases and the indoor air temperature is lower. Consequently, the ventilation heat losses are reduced and the effective heat storage capacity is improved [6] [9] [10] [11].

As mentioned before, the thermal inertia sets the heat storage capacity of the built environment. The building thermal inertia is typically mainly provided by the dense construction elements present in the structure of the edifice. One solution to further increase the building thermal storage capacity is to employ phase change materials (PCMs) which can offer an appreciable energy storage density within narrow temperature span. Latent heat thermal energy storage (LHTES) can be integrated in the inner surfaces of the indoor space in order to increase the thermal inertia of light structure buildings. Some researchers demonstrated the benefit of PCM wallboards and PCM UFH for space heating load shifting with set point temperature modulation control [12] [13]. In addition, furniture pieces present a large surface area exposed to the indoor environment. It can also be used for the integration of PCMs and thus extend the applicability of the TES strategy [14].

Even if regulations tend to improve the energy efficiency of buildings, the heating demand remains dominating in cold winter countries. In Denmark, for example, 25% of the annual national energy use is dedicated to heating up buildings [15]. Moreover, single family houses represent 60% of the heated area of Danish residential buildings [16]. This paper will thus focus on the capacity of single family dwellings to shift in time their indoor space heating energy use by the means of set point temperature modulation under Danish weather conditions. Although similar investigations have been conducted for other countries, the current numerical study aims at quantifying more precisely the influence of the different main building parameters in the Danish context. Moreover, this paper is the first one to explore the implication of additional indoor thermal mass from phase change materials and furniture elements regarding indoor space heating energy flexibility of buildings. A better understanding of the building thermodynamics and its thermal storage abilities will help improving the accuracy of building simulation tools and ease the investigations on demand side management and energy flexibility strategies.

Firstly, the methodologies for calculation of the energy flexibility factor and the building thermal inertia are explained. The different study cases and the numerical building model and its sub-components are then presented in details. A discussion follows about the results of this numerical investigation, including a parametric sensitivity analysis. Finally, a conclusion and suggestions for further research close the article.

2. Methodology

2.1. Definition of the building energy flexibility

With the recent paradigm shift in the building energy research sector from energy efficiency to demand-side management, several different energy flexibility indicators have been created. A review of these different metrics has been published by Rui et al. [17] and Reynders et al [18] . However, there is presently no scientific agreement about a clear definition of what is the "building energy flexibility". Consequently, there is no standard way to assess it. The on-going IEA EBC Annex Project 67 [19] [20] is aiming to tackle these two problems by providing guidelines and increasing knowledge on the building energy flexibility concepts.

In this study, the approach is similar to the one of a recent publication by Le Dréau et al. [9]. The energy flexibility is defined as the ability for the building to minimize the heating energy usage during high price periods and maximize it during low price periods. In other words, the building energy flexibility index assesses the capacity to shift in time heating use from high price to low price periods whilst insuring good indoor thermal comfort (see example on **Fig. 1**). The flexibility index is calculated according to equation (1). It represents the change of heating use during medium and high price periods when the energy is accumulated during low price periods compared to a reference scenario without any thermal storage strategy.

$$\boldsymbol{F = \left[\left(1 - \frac{\%High}{\%High_{ref}}\right) + \left(1 - \frac{\%Medium}{\%Medium_{ref}}\right)\right] \times \frac{100}{2}} \qquad (1)$$

Where $\%High$ and $\%Medium$ are the percentages of yearly heating energy (relatively to the total yearly heating needs) used during high and medium price periods respectively when the heat storage strategy is operational. Equivalently, $\%High_{ref}$.and $\%Medium_{ref}$ are the percentages of yearly heating energy for the reference scenario (no heat storage strategy). The flexibility index takes the value of zero if the repartition of the energy use is the same as in the reference case. The building did not provide any energy flexibility. The index becomes negative if the share of high and medium price periods is larger than the reference values. In that case, the building is performing worse than the reference scenario in terms of energy flexibility. The flexibility index reaches 50% if the energy share of the medium price period does not change and if all the energy share of the high price period is shifted to the low price period. Similarly, the flexibility index reaches 50% if the energy share of the high price period does not change and if all the energy share of the medium price period is shifted to the low price period. If both the high and the medium price period shares are decreased by half, the flexibility index also takes the value of 50%. If there is no remaining energy usage during the periods of high and medium price, the flexibility index takes the maximum value of 100%. In that situation, the building presents a total energy flexibility.

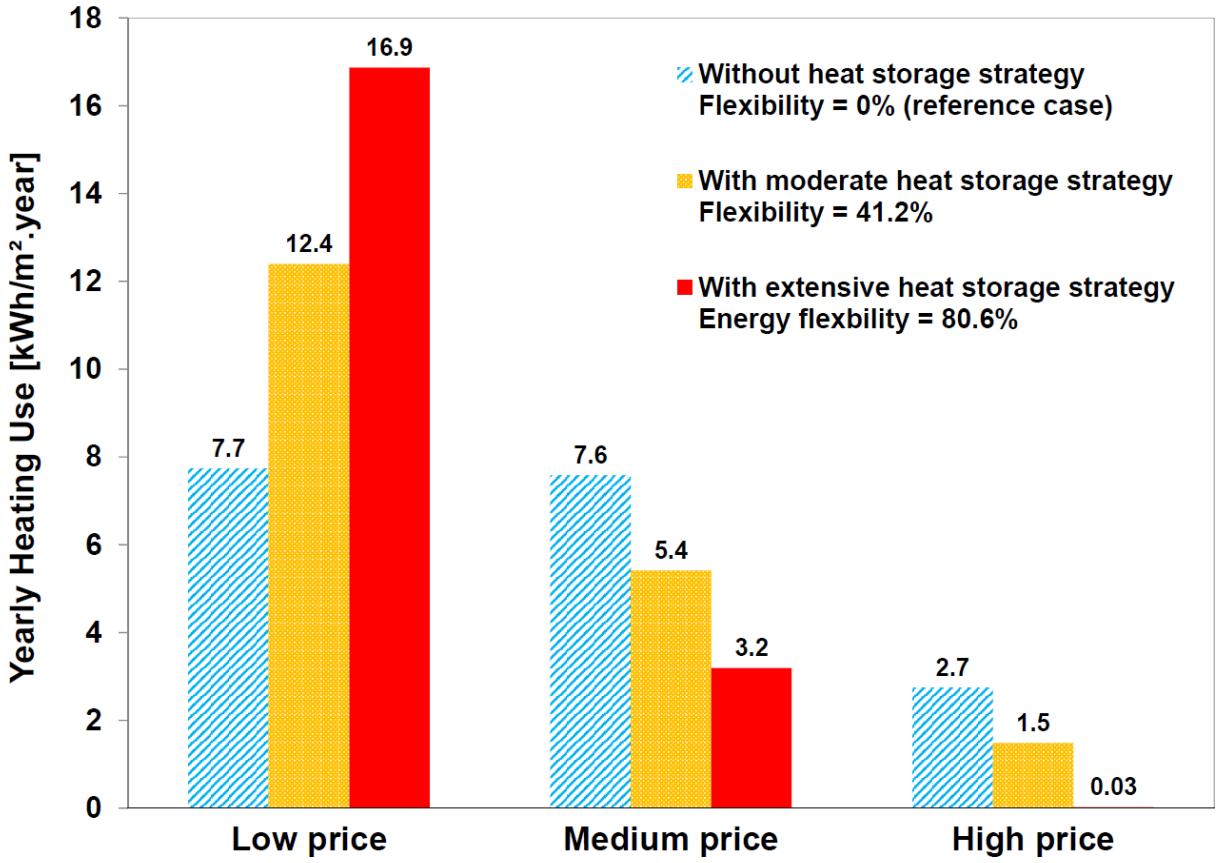

Fig. 1. *Variations of yearly heating use for light structure passive house with heat storage strategy (results from the current study).*

Several comments can be made about the definition of this flexibility factor. Firstly, it is necessary to obtain a reference energy usage scenario of the building to calculate its flexibility factor. Secondly, the energy price categories are established with an arbitrary definition (see following section) and are based on a specific electricity spot price profile. Different spot price profiles with shorter or longer price periods can have a significant impact on the flexibility factor calculation results. Similarly, the building's local climate and occupants' behaviour can largely influence the building energy flexibility potential [21].

2.2. Evaluation of the thermal inertia of building components with PCM

As this numerical study pays particular attention to the different types of thermal mass elements in dwellings, it is important to assess the thermal inertia of each building component in a consistent way. The "effective thermal inertia" (expressed in J/K.m² or in Wh/K.m²) is therefore chosen as a common metric for the different construction elements. This metric is not present in the numerical model, but only used to compare the study cases.

The effective thermal inertia of a building element can be evaluated numerically for different variation periods; typically 1 hour (hourly effective thermal inertia) or 24 hours (daily effective thermal inertia) [22]. Because the most important boundary conditions driving the transient response of a building (outdoor temperature, solar radiation, internal load, etc) present a clear daily variation profile, it is very common to characterize the building effective thermal inertia with a 24 hours variation periods, which is the case in the current study.

The total daily effective thermal inertia of a building is calculated as the sum of the daily effective thermal inertia of each of its construction component, including internal partition walls. For the sake of convenience, in the rest of this article, the total daily effective thermal inertia of the building study cases is reported with respect of the gross floor surface area of the house and noted "building thermal inertia" (Wh/K.m²).

The calculation of the daily effective thermal inertia of planar building elements can be performed according to the detailed matrix method described in the standard EN ISO 13786 [22]. This matrix method is based on the quadrupole formalism presented by Maillet et al. [23]. It is straightforward and can easily be implemented in calculation software to evaluate multi-layered material elements. However, it is based on the analytical solution of a simplified thermodynamic system assuming one-dimensional heat transfer through infinitely large planar solids. The dynamic boundary conditions are restricted to following a sinusoidal function. This assumption is nonetheless reasonable as sinusoidal functions are a common way to model indoor and outdoor temperature time variations [24]. For a given surface orientation and exposure, the surface heat transfer coefficient is assumed to be constant. The latter is set according to common values used in building energy calculations [25]. Another limitation of this methodology is that it only considers materials with constant thermal properties. Consequently, it cannot be used for materials in which phase transition occurs.

In order to evaluate the effective thermal inertia of building elements including PCM, a one-dimensional finite volume method (FVM) numerical model of the planar element with PCM layers is developed (see description of the models for building elements with PCM in the following sections). It is then used for the calculation of the total internal energy variations when dynamic boundary conditions are applied. Kuznik et al. [24] employed a similar approach for the optimization of a PCM wallboard. From the point of view of a single side of the planar element, its areal effective thermal inertia κ (J/K.m²) is the capacity to store energy when subjected to periodically variating boundary conditions [22]. It is equal to the amplitude of internal energy variation ΔE (Joule) of a half volume element divided by the amplitude of temperature change $\Delta\theta$ (K) at the boundaries, and the element's surface area A (m²):

$$\boldsymbol{\kappa = \frac{\Delta E}{\Delta\theta \times A}} \qquad (2)$$

Similarly to the matrix method for daily effective thermal inertia calculation, a 24-hour period sinusoidal function is used to define the boundary conditions. The average boundary conditions temperature is equal to the melting/solidification temperature of the PCM. Once the system reaches periodic steady state, the areal effective thermal inertia is calculated. This numerical method has been validated against the detailed matrix method for common building materials and shows very good agreement. More information about the numerical method used to assess the effective thermal inertia of PCM elements can be found in a detailed technical report [37].

3. Description of the building study cases

A single-story building with 126 m² of heated space and a typical geometry for dwellings in Denmark is chosen as base case study. As the structural thermal inertia, the additional indoor thermal mass, the envelope performance level and the heating system type are under study in this paper, a total of 144 different versions of the single family house presented on **Fig. 2** are generated with variations of these four building parameters.

Two categories of building envelope performance are considered; namely, low-insulation house from the 80's and high-insulation passive house. The low-insulation case corresponds to a Danish house built in the years 1980 with relatively poor thermal performances: yearly heating need around 160 kWh/m². The high-insulation case corresponds to a "KomfortHus" and has been designed according to the Passive House standard [26]: yearly heating need around 13 kWh/m². For both categories, the insulation thickness and thermal conductivity, the infiltration and ventilation rate, the windows' characteristics and surface area, and the HVAC systems' performance are chosen accordingly.

The material properties of the external and internal surfaces of the house's walls, ceilings and floors are set in order to generate three structural thermal inertia building classes with three sub-variations in each of them. The three main categories of structural thermal inertia have been chosen according to the recommendations of national and international standards [27] [28]. This effective structural thermal mass variation range is representative of the different heat storage capacity encountered in residential buildings:

- Light-weight structure house; building thermal inertia: 30 Wh/K.m², 40 Wh/K.m² and 45 Wh/K.m².
- Medium-weight structure house; building thermal inertia: 50 Wh/K.m², 60 Wh/K.m² and 70 Wh/K.m².
- Heavy-weight structure house; building thermal inertia: 90 Wh/K.m², 100 Wh/K.m² and 110 Wh/K.m².

In addition, four indoor thermal mass configurations are considered: empty rooms filled with air only; additional indoor items/furniture present in the rooms; PCM integrated in furnishing elements; PCM wallboards placed on the inner surfaces of the house's walls and ceilings.

Finally, two types of heating system are integrated in the different building scenarios: convective radiator (30% of heat output by radiation and 70% by convection) and water-based under floor heating system. The design of the heating systems has been made according to the Danish and international standards and manufacturer's technical guidelines

[29] [30] [31] [32] [33] [34]. It is assumed that the primary energy source of the heating system is electricity with the use of a heat pump for example.

The outdoor conditions correspond to the typical weather data in Denmark (Danish Design Reference Year 2013) [35]. The buildings are therefore assumed to be located in an open field around Copenhagen. People load and equipment internal gains are set according to a typical Danish appliance usage and dwellings occupancy schedule for four habitants [36]. Each thermal zone has a specific people and equipment load schedule depending on the type of room (living room, kitchen, bedroom or bathroom). However, the indoor temperature set point is defined on the building level. In the case of set point modulation control, it implies that the indoor temperature of the whole house is adjusted independently of whether a room is occupied or not.

The main information about the building cases is summarized in **Table 1**. More details can be found in a technical report [37].

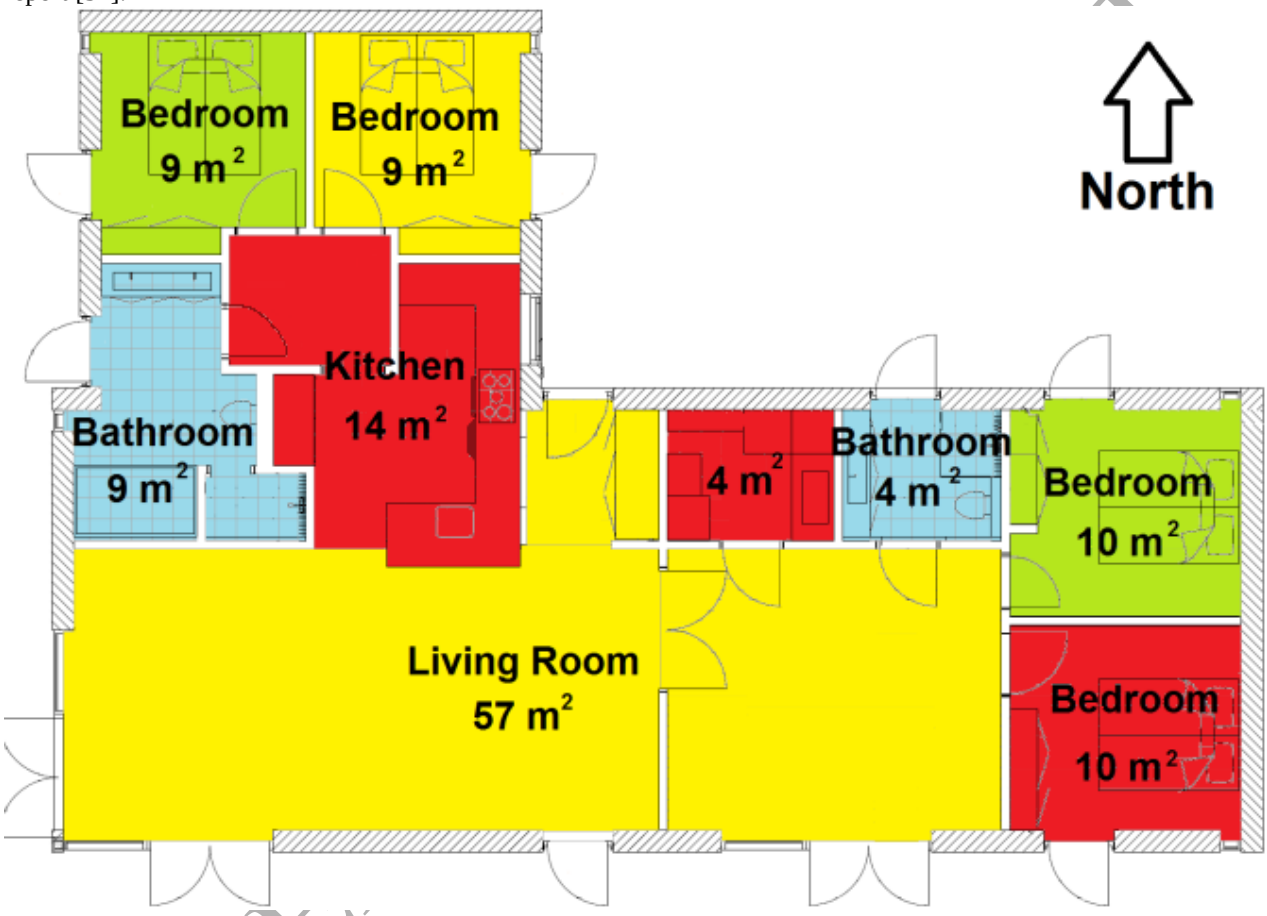

Fig. 2. *Plan view of the house case study.*

Building envelope category	House 1980's			Passive House		
Structural thermal mass category	Light	Medium	Heavy	Light	Medium	Heavy
Effective thermal mass: Cm 24h ($Wh/K.m^2$ gross floor)	30 - 40 - 45	50 - 60 - 70	90 - 100 - 110	30 - 40 - 45	50 - 60 - 70	90 - 100 - 110
Building envelope heat losses ($W/K.m^2$ gross floor)	1.12	1.13	1.13	0.37	0.37	0.37
U-value windows ($W/m^2.K$)	1.7			0.78		
g-value windows (-)	0.63			0.5		
Ratio windows / gross floor area (m^2)	16.70%			26.90%		
Windows area (m^2)	25.1			40.39		
Air infiltration (ACH)	0.2			0.07		
Ventilation (ACH)	0.4			0.4		
Heat recovery (-)	0			0.8		
Air flow heat losses (W/K)	64			15.6		
Air flow heat losses ($W/K.m^2$ gross floor)	0.43			0.1		
Yearly radiator heating need with set-point at 22°C (kWh/m^2 net floor.year)	164	160	155	14	13	12
Maximum radiator heating power (W/m^2)	75			25		
Under-floor heating type	Type G wood floor	Concrete screed	Concrete screed	Type G wood floor	Concrete screed	Concrete screed
Yearly under-floor heating need with set-point at 22 °C (kWh/m^2 net floor.year)	160	151	157	15	13.5	13
Nominal water flow per UFH loop (l/h)	170			125		
UFH maximum inlet water temperature (°C)	47	43	43	35	30	30

Table 1*: Characteristics of the building cases.*

4. Description of the building numerical model

Within the framework of the EnovHeat project [38], a detailed (white box) multi-zone building energy model of a single family house has been developed. This model is used in the present study. The following section presents succinctly the different elements of the MATLAB - Simulink numerical model and the main results of the validation test procedures. More information about the building model and all validation test results can be found in a detailed technical report [37].

4.1. Multi-zone building model

Similarly to the HAM-tools [39] the heat transfer through planar construction elements is calculated with a one-dimensional finite control volume method (FVM) with explicit formulation comprising a small number of control volumes (commonly named “Resistance-Capacitance network” or “RC network”). External wall, internal wall, ceiling and roof elements are subdivided into 5 thermal nodes along the direction normal to the main plan surface: 1 node for the external cladding (plaster, wood, brick or concrete), 1 node for the internal cladding and 3 nodes for the insulation layer (mineral wool). Floor elements (including the soil layer under the house, the expanded polystyrene insulation layer and the concrete or wood slab containing the UFH system) are subdivided into 9 nodes: 3 nodes for the soil layer, 3 nodes for the insulation layer and 3 nodes for the concrete or wood slab. The number of nodes in the different construction layers (spatial discretization refinement) is chosen as a compromise between model complexity, computation time and accuracy. For studying the indoor space thermodynamics, a proper modelling of the interior surfaces on the inner side of the insulation is important [40]. Because the Biot number of the inner cladding layers is smaller or close to 0.1, it is considered that the single lumped capacitance assumption is reasonable. However, for the floor elements, the hydronic under-floor heating system embedded in the upper concrete screed / wooden slab highly

activates the thermal mass of the latter. In order to accurately model the dynamics of the floor systems, the spatial discretization is thus refined to 3 nodes for the concrete screed / wooden slab.

For the external surfaces, the direct and diffuse solar radiation and the long-wave radiation to the sky are calculated as a function of the local weather conditions and the surface orientation. Inside each thermal zone, the inner surfaces and the indoor air temperature nodes are connected within a star network configuration with constant mixed convection/radiation surface thermal resistance coefficients. Thermal bridges, ventilation, air infiltration and windows heat losses are modelled using constant thermal resistances. The ventilation heat recovery is activated during the heating season and turned off for an air inlet temperature above 22 °C. In case of over-heating during summer period, natural ventilative cooling is simulated by increasing the ventilation rate without any heat recovery.

70% of the people load and equipment internal heat gains are considered fully convective and therefore applied directly to the air node of the thermal zone. The remaining 30% are modelled as radiative and distributed over all the indoor surfaces with respect to their surface area. Concerning the internal solar loads, 15% are modelled to go directly to the air node, 55% to go to the floor and 30% to go to the vertical walls of the thermal zone [41].

The 10 different thermal zones of the dwelling (9 rooms and an attic) are connected together to form the house multi-zone model. Doors in between the rooms are considered closed all the time and therefore there is no direct air exchange between the different thermal zones. Because the heat equation is solved with an explicit scheme, the simulation time step size is chosen to be 60 seconds in order to avoid numerical instability.

4.2. Heating systems

Two types of heating emitters are investigated in this study: convective radiator and water-based under floor heating system. The paper focuses on the house heating demand and therefore only considerers the emitted energy and not the total energy consumption of the system. Consequently, the primary systems for heat generation are not modelled.

The radiator heating system is modelled with a first order transfer function which has a time constant of 10 minutes [42]. The radiator is regulated by a PI controller and emits 30% of its heat output by radiation and 70% by convection.

The water-based UFH system is modelled as a horizontal heat exchanger embedded in a slab by coupling a “plug flow” model in a pipe with the ε-NTU method. The plug flow principle model accounts for the dynamics of the uncompressible brine moving inside a pipe at variable flow rate. At each time step, an additional fluid cell is queued and pushed at the inlet/beginning of the pipe. The size of this new fluid cell is calculated according to the brine volume flow rate and the diameter of the pipe. Because of conservation of the total volume in the pipe, all the other queued fluid cells are pushed forward towards the pipe’s outlet. The outlet fluid temperature is calculated as the volume-weighted average temperature of the fluid cells exiting the pipe at each time step. The plug flow model assumes a no-mixing condition between adjacent fluid cells. This is a reasonable assumption as the brine is circulating with a fairly high velocity in the pipes and the temperature difference between each cell remains small. Therefore the fluid cells solely exchange heat by convection with the walls of the surround pipe [43]. The ε-NTU method is used to calculate the heat transfer between each fluid cell in the pipe and the walls of the pipe and, consequently, with the rest of the UFH slab. This methodology collapses the complex heat transfers in the three-dimensional domain of a horizontal embedded heat exchanger into a simplified one-dimensional Resistance – Capacitance star network. The effectiveness of the heat exchanger takes into account the equivalent interaction thermal resistance in the layer of the slab where the water pipes are laid [32] [44]. The convective heat transfer coefficient of the brine in the pipe is calculated according to the fluid velocity, Reynolds number, temperature and other temperature dependent thermo-physical properties. The conductive slab surrounding the UFH pipe circuit is sub-divided into 3 thermal nodes. A PI controller regulates the water temperature provided to the UFH distribution manifold.

4.3. Latent heat thermal energy storage

Phase change materials have found interesting applications for TES in buildings. One of the most promising solutions is the integration of PCM in wallboard panels on the internal surfaces of the indoor environment such as walls and ceilings. Moreover, the large surface area of furnishing elements which are exposed to the indoor environment is also a good candidate for the integration of PCMs [14].

Many LHTES numerical models for building systems are using an apparent heat capacity function to account for the latent heat of the phase transition. However, this approach does not really represent the physics of the PCM but only its apparent behaviour with regards of temperature. The PCM model for this study is based on an enthalpy formulation which really simulates the melting/solidification phase transition process at constant temperature [45] [46].

The stable form PCM is considered to be a homogenous material set in thin layers so that the heat transfer can be assumed one-dimensional. Density, specific (non-latent) heat capacity and thermal conductivity of each control volume are calculated as function of its current temperature. These material properties and melting/solidification temperatures are used to build an enthalpy/temperature function curve. A fully implicit one-dimensional FVM formulation with 1 mm thick control volumes performs the heat transfer calculation in between the PCM layers. The variation of internal energy in each control volume is then used with the enthalpy/temperature function to get the corrected temperature.

One limitation of this numerical model is that it cannot account for multiple phase transition temperatures. This situation can occur for PCMs which are made of several compounds with dissimilar melting temperatures. It is thus assumed that the PCM has only one specific melting temperature and one specific solidification temperature. These temperatures can be different to take into account hysteresis phenomena. However, in this model, it is chosen to not introduce any hysteresis effect and therefore both melting and solidification temperatures are fixed to 22 °C.

Two types of LHTES system are tested in this study: PCM wallboards for the inner surfaces of walls and ceilings, and PCM integrated in furniture elements. Both systems consist of Energain® stable form PCM arranged in thin slabs. Energain® is a well-known commercial product. It is composed of 60 w% micro-encapsulated paraffin (organic PCM) mixed with 40 w% polyethylene [47]. The thickness of the PCM panel is chosen to be 1.5 cm. This value seems to be a reasonable choice to insure a significant increase of the heat capacity for daily temperature variations with an optimum amount of material [37].

Guarded Hot Plate Apparatus and Differential Scanning Calorimetry measurements have been conducted in order to determine precisely the thermal characteristics of the Energain® product. Some dissimilarity has been found between the current measurements and the results from a previous study of Kuznik et al. [24]. This discrepancy is probably due to the variability of the Energain® manufacturing process. Based on these experimental data and the information provided by the manufacturer, realistic PCM parameters (presented in **Table 2**) are chosen for the LHTES systems which are implemented in the building model. In particular, the PCM thermal conductivity is constant at 0.22 W/m.K for temperatures below 16 °C, constant at 0.18 W/m.K for temperatures above 28 °C, and varies linearly from 0.22 W/m.K to 0.18 W/m.K within the temperature range of 16 °C to 28 °C.

The additional daily effective thermal inertia of the PCM integrated in furniture elements is around 71.4 Wh/K.m² of gross floor surface area in average. The additional daily effective thermal inertia of the PCM wallboards ranges from 6.4 to 68 Wh/K.m² of gross floor surface area. It should be noted that the large range of additional thermal inertia from the PCM wallboard is due to the fact that the latter increases significantly the thermal mass of light-weight structure walls but is almost ineffective when placed over heavy wall elements such as concrete masonry or bricks.

	PCM characteristics
Paraffin mass content (%)	**60**
Paraffin latent heat of fusion (kJ/kg)	**200**
Melting temperature (°C)*	**22**
Thermal conductivity (W/m.K)*	**0.22 – 0.18**
Density (kg/m³)*	**1000**
Specific heat capacity (J/kg.K)*	**2000**
Latent heat of fusion (kJ/kg)*	**120**
Total heat storage for $\Delta\theta$ = 30 K (kJ/kg)*	**180**

* For stable form PCM product: 60 w% paraffin in polyethylene matrix

Table 2*: Characteristics of the phase change material.*

4.4. Indoor items/furniture elements

The additional thermal mass of the indoor items and furniture elements inside occupied buildings can be accounted in different ways with various degrees of details: from simple virtual thermal node aggregating all elements, to detailed modelling with explicit location of each item in the building space [14] [48]. In the current study, the additional indoor thermal mass is modelled as an equivalent fictitious planar element which aggregates all indoor items into an homogenous representative material. This approach is rather simple to implement in a building model. It has been found to be valid compared to more complex models with explicit geometries and locations of the indoor content [49]. The thermo-physical properties of this equivalent element are chosen according to a previous study on the indoor content of dwellings in Denmark [14] and are presented in **Table 3**. The thermodynamics of the equivalent planar element is calculated with a one-dimensional fully implicit FVM model comprising control volumes with 1 mm thickness.

In each of the dwelling's thermal zones, the indoor thermal mass element is 60 kg/m² of the room's floor surface area concentrated in a 4.7 cm thick slab. Consequently, the surface area of one side of the planar element is equal to 1.8 times the room's floor surface area. The equivalent planar element does not have any real geometrical representation or position in the room. However, a previous publication showed that items in the built environment can account for a large share of the indoor surfaces exposed to radiations [14]. It is therefore assumed that 50% of the radiative share of the equipment, people, solar and radiator heating loads are absorbed by these elements' surfaces.

The element is coupled to the rest of the thermal zone in the same way as if it was an additional internal wall. The mixed convection/radiation surface thermal resistance coefficient is set constant and equal to 0.13 m².K/W. The additional daily effective thermal inertia of the equivalent element is around 18.1 Wh/K.m² of gross floor surface area in average.

In the case of PCM integrated on furniture elements, the two models for indoor thermal mass/furniture and for PCM are combined together. The 1.5 cm thick layer of Energain® stable form PCM is added on the upper part of the equivalent furniture planar element.

	Equivalent planar element
Thickness (mm)	**47**
Density (kg/m³)	**715**
Thermal conductivity (W/m.K)	**0.3**
Specific heat capacity (J/kg.K)	**1400**
Space discretization (nodes)	**20**

Table 3*: Equivalent indoor thermal mass/furniture properties.*

4.5. Validation of the numerical models

As discussed before, the spatial discretization of the different building elements has been chosen as a compromise between model complexity, computation time and accuracy. The simulation time step size is fixed to 60 seconds to avoid numerical instabilities [50]. The MATLAB-Simulink one-dimensional FVM formulation for the construction elements has been compared against an analytical solution in the case of steady state boundary conditions. The average absolute difference between the analytical solution and the MATLAB-Simulink model is 0.0015 °C. The latter has then been compared to the commercial software BSim in the case of dynamic boundary conditions (varying temperatures, solar radiation, wind and long-wave radiation). The average absolute temperature difference between the MATLAB-Simulink model and the BSim reference model is 0.3 °C. The entire MATLAB-Simulink multi-zone model of the case study house has then been compared against a BSim reference model of the same building. The average absolute difference between the MATLAB - Simulink model and the BSim reference model is 0.12 °C for indoor temperature, 0.5 W/m² for the heating power need and 0.88% for the cumulative energy consumption over 2000 hours of the heating period. In addition, a BESTEST procedure has been performed with test cases presenting different orientations, insulation levels, structural thermal inertias and with a variable temperature set point. It is shown that the MATLAB – Simulink building model produces calculation results (indoor temperature and the heating/cooling needs) which are always in between the extrema of the other benchmarked simulation tools [37].

Similarly, the MATLAB – Simulink hydronic under-floor heating system model is compared against a BSim reference model with steady state boundary conditions. The average absolute temperature difference between the two models is 0.07 °C. The MATLAB – Simulink model is then tested in heating and cooling mode in a room with dynamic boundary conditions and compared to the BSim reference model. The average absolute difference between the two models regarding heat transfer, room air temperature and pipe level temperature is 3.2 W, 0.07 °C and 0.1 °C respectively [37].

As mentioned before, the equivalent fictitious planar element modelling method is adequate for simulating additional indoor items in the indoor environment. The MATLAB – Simulink one-dimensional implicit FVM model representing this element is compared against analytical solution in the case of steady state boundary conditions, and against the commercial software COMSOL Multiphysics in the case of dynamic boundary conditions. The temperature difference between the MATLAB – Simulink model and the analytical solution is in the order of 10^{-8} °C. The temperature difference between the MATLAB – Simulink model and the COMSOL reference model with dynamic boundary conditions is below 0.02 °C most of the time [37].

Finally, The PCM model integrated in the building elements has been compared against experiment tests performed on three PCM commercial products with a Guarded Hot Plate Apparatus. The dynamic tests show that the MATLAB – Simulink model can simulate properly the PCM thermodynamics with a 0.2 °C temperature accuracy most of the time. However, at lower temperatures, the numerical model presents some discrepancies with the experimental tests. This is due to the fact that the tested paraffin-based PCM products have a residual phase transition at temperatures much lower that the stated main transition temperature. The current PCM model used in this study cannot account for additional phase transitions and is thus limited to a single phase transition at a fixed temperature [37].

4.6. Heat storage control strategy

The indoor space heat accumulation strategy which is implemented in the building model is the same as the one used by Le Dréau et al. [9] and similar to the one of Péan et al. [51]. In principle, the end-goal of the energy flexibility and demand-side management strategies is to allow the integration of a larger share of intermittent RES in a Smart Grid system. For that purpose, the building should be able to accumulate energy when there is an excess of RES production, and reduce its energy usage when the RES production is low. In countries like Denmark, where a large share of the electrical energy production mix is coming from wind turbines, the electricity spot price is a good indicator of the RES availability and the energy demand. Consequently, the Danish electricity spot price (hourly market price observed in the Nordic electricity market "Nord Pool" in the year 2009 [52]) is used here to control the heating modulation strategy. The building accumulates heat energy during low price periods and save heat energy during high price periods.

As shown on **Fig. 3**, limits for low price and for high price are calculated every hour as the lowest and highest quartile of the electricity market price over the last 14 days. The house temperature set point is then modulated accordingly with three different values: minimum set point of 20 °C, neutral set point of 22 °C and a maximum set point of 24 °C. The temperature span between the minimum set point and the maximum set point is 4K. It corresponds to a normal level of thermal comfort with less than 10% of unsatisfied occupants [53]. Moreover, the transient indoor temperature change is always kept below the thermal comfort limit of 2.1 K/h [54]. When the spot price becomes low, the set point is increased to accumulate heat energy. When the spot price becomes high, the set point is decreased to save heat energy. When the spot price is within the medium category, the set point is kept at 22 °C.

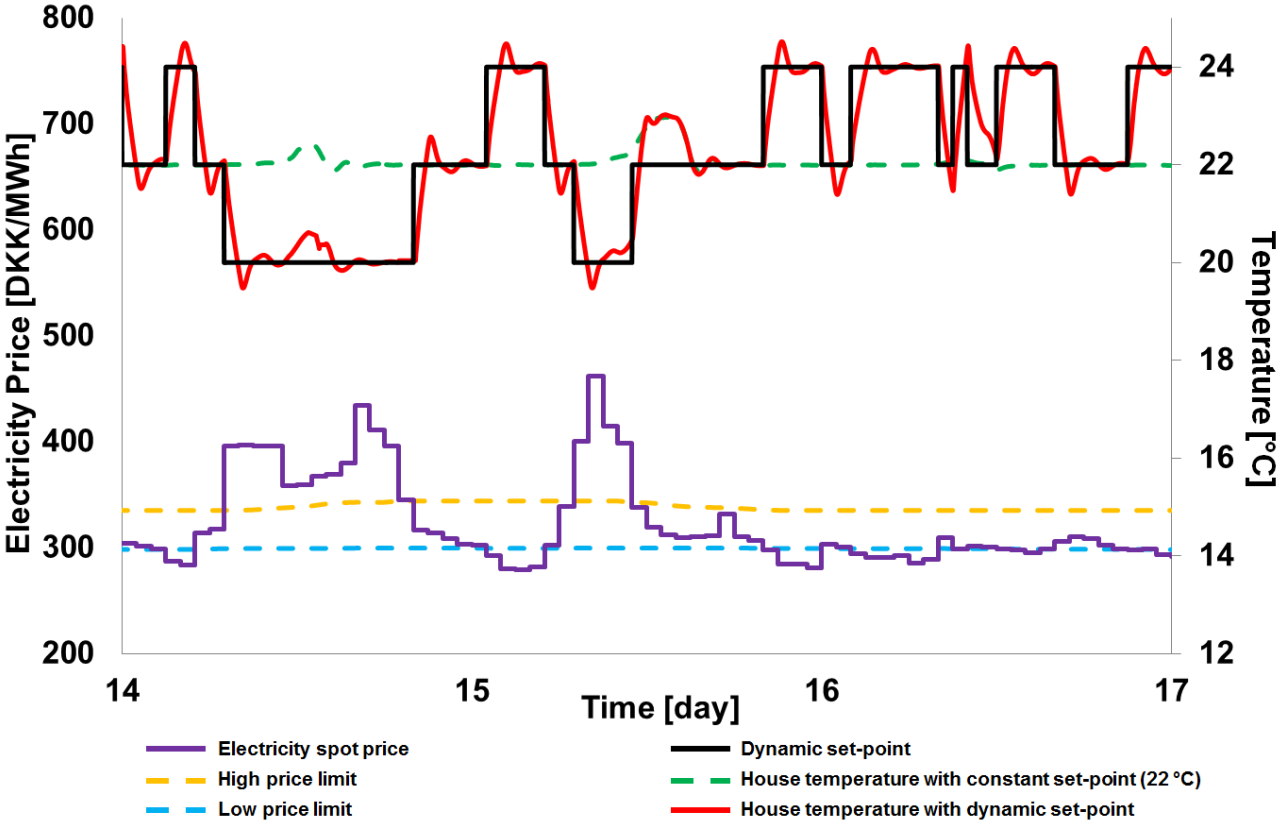

Fig. 3. *Temperature set point modulation with price control and maximum activation time of 6 hours for low-insulation light structure house with radiator.*

However, the occupants of a building might not necessary accept the change of the indoor temperature set point for an extended period of time based on an external signal. The longer the set point temperature is away from the neutral level and the more disturbance could be induced to the occupants. In order to study the impact of different occupants' disturbance levels on the building energy flexibility, a maximum activation time is defined between 30 minutes and 24 hours. When the low or high activation period reaches the maximum activation time, the set point is put back to its neutral level of 22 °C. The temperature set point is then maintained at the neutral point for a duration equal to the maximum activation time before the same activation can occur again [9].

5. Results and discussion

5.1. Impact of additional indoor thermal mass on the building time constant

The impact of additional indoor thermal mass on the building's dynamics is investigated. Firstly, the time constant of six building cases from the three different structural thermal mass classes (light: 30 Wh/K.m², medium: 50 Wh/K.m², heavy: 100 Wh/K.m²) and the two envelope performance categories (low-insulation house from the 80's, high-insulation passive house) is calculated without any additional indoor thermal mass. The outdoor temperature is kept constant whilst all radiation and internal gains are set to zero. Once the house's temperature has reached a steady state (indoor temperature set point at 19 °C), the convective radiator power is increased to maximum until the temperature reaches a new steady state. The building time constant is then calculated as the time needed to reach 63.2% of the temperature change between the two steady states [55].

The **Fig. 4** presents the influence of the different types of additional thermal mass on the building's time constant compared to the empty room reference cases. The time constant and the thermal inertia of the reference empty buildings are stated in the table below the figure. One can observe that the PCM wallboards and the PCM integrated in the furniture increase significantly the time constant of all the buildings. Concerning the indoor items/furniture elements, their effect is limited for medium and heavy structure cases but not negligible for light structure buildings.

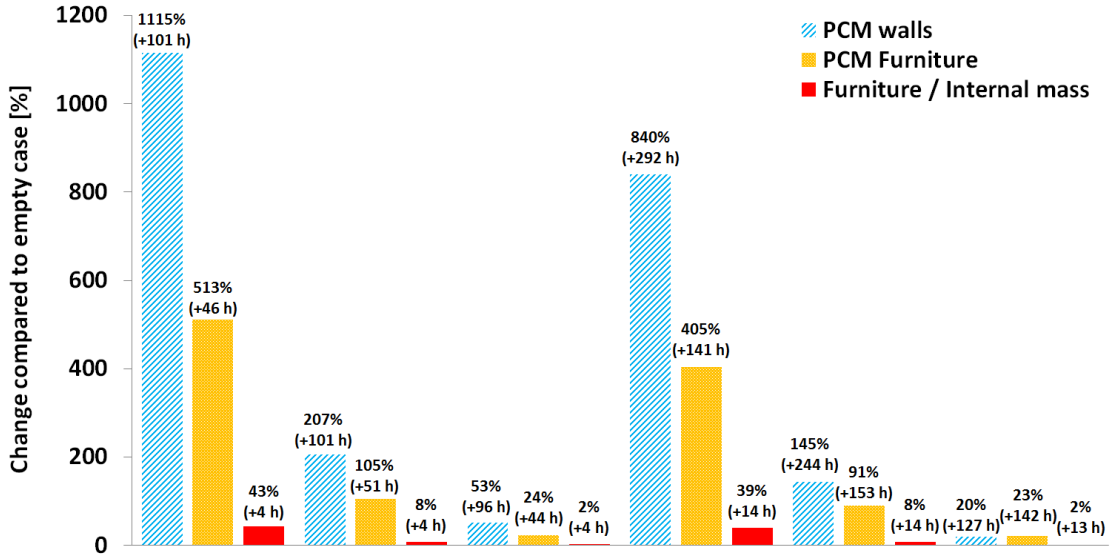

	Light House 1980	Medium House 1980	Heavy House 1980	Light Passive House	Medium Passive House	Heavy Passive House
Empty building time constant [hours]	9	49	181	35	169	626
Empty building thermal inertia [Wh/K.m²]	30	50	100	30	50	100

Fig. 4. *Change of building time constant with additional internal thermal mass.*

5.2. Influence of the maximum activation time on the building energy flexibility

48 different building configurations (two envelope performance categories, three structural thermal mass classes, four kinds of additional indoor thermal mass and two types of heating system) are then simulated with 8 different maximum activation times for the heat storage strategy. As mentioned before, the calculation of the energy flexibility index requires a reference building case. The house scenario without heat storage control strategy is used as reference. One can see on **Fig. 5** some examples of the evolution of heating energy use distribution over the different price categories when the maximum activation time for TES is increasing. The control strategy tries to maximize the energy use during low price period and minimize it during high price period. However, there is no particular action to decrease energy consumption during medium price period. Consequently, the accumulated thermal energy is firstly impacting the high price category and marginally decreasing the medium price category in a second time. Similar patterns can be observed for all the building cases.

Thermal storage in the built environment is necessarily imperfect and increasing the indoor temperature set point induces an augmentation of the building heat losses through the envelope and ventilation system. It is therefore normal to observe a slight increase of the yearly heating energy use in study cases employing heat accumulation strategy. For 24 hours of maximum activation, the average increase of the heating use of houses from the 80's and passive houses is 3.3% and 6.3% respectively. These observations are in agreement with previous studies [9].

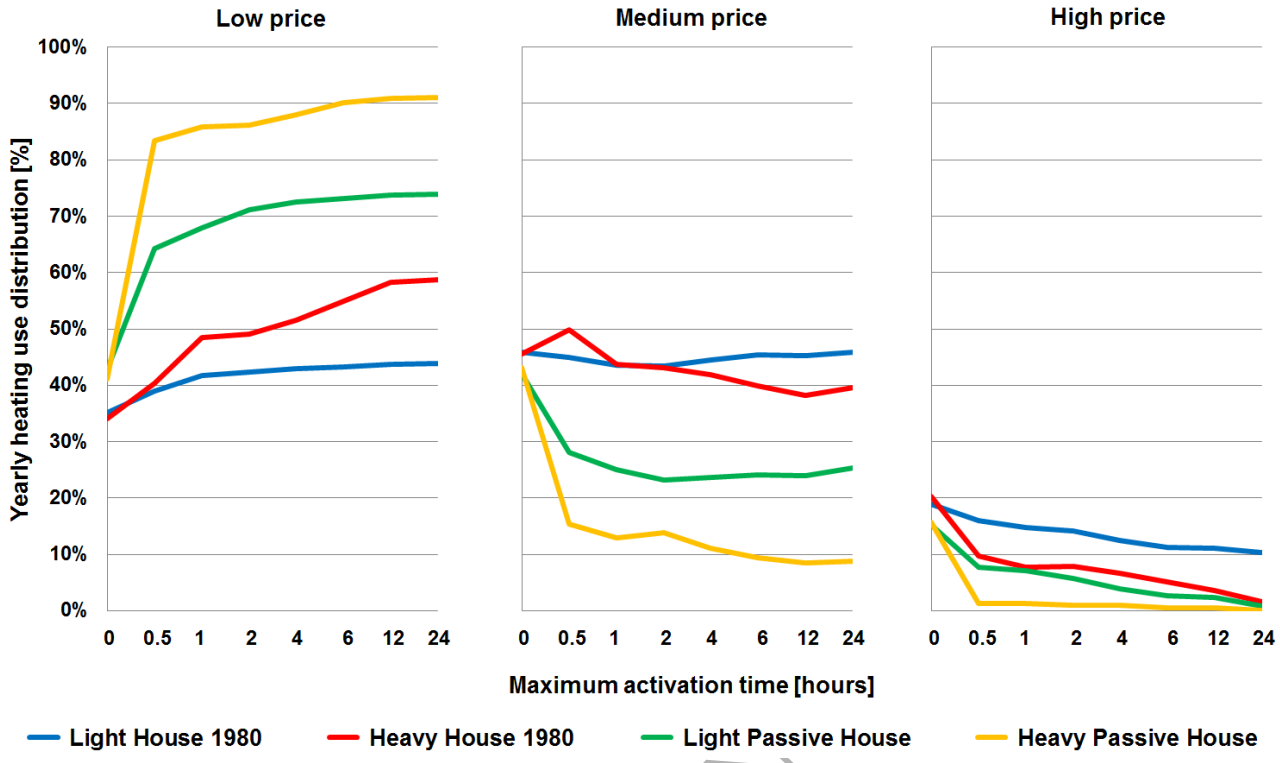

Fig. 5. *Examples of the yearly heating use distribution variation for different TES maximum activation times (building examples are equipped with radiators and are without additional indoor content; the 0 hour maximum activation time cases correspond to the reference scenario without heat storage strategy).*

Fig. 6 shows the evolution of the building energy flexibility index as function of the maximum activation time. These results are coherent with the previous study of Le Dréau et al. [9]. The flexibility index increases quickly and then stabilizes for maximum activation times above 6 hours. This saturation effect can be explained by two phenomena. First of all, the effective building thermal storage ability reaches its maximum limit and accumulating more energy is ineffective to improve flexibility. Secondly, the indicated maximum activation time is different from the effective activation time due to the variation frequencies of the price signal. A Fourier analysis (frequency spectrum analysis) of this price signal shows that its main components have an oscillation period of 12 hours, 24 hours and 1 week. Consequently, the low price periods for energy accumulation are rarely lasting more than 6 hours before the price signal rises to medium or high price periods. It means that even if the maximum activation time for energy storage is 24 hours, the effective activation time rarely reaches such duration because low price periods are usually much shorter. One can see on **Fig. 7** that the average effective yearly activation time plateaus at 4.7 hours.

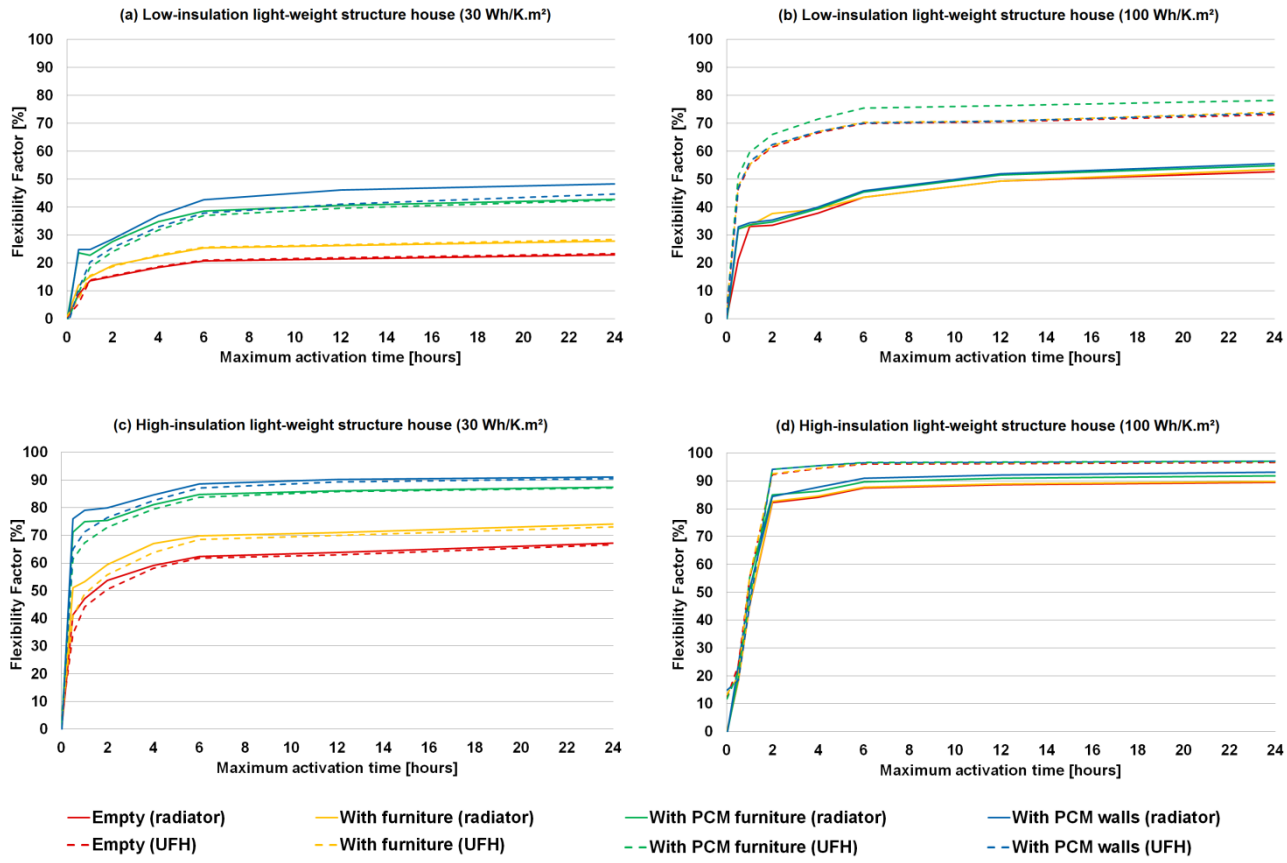

Fig. 6. *Building energy flexibility as function of maximum activation time (radiator: convective radiator; UFH: under floor heating).*

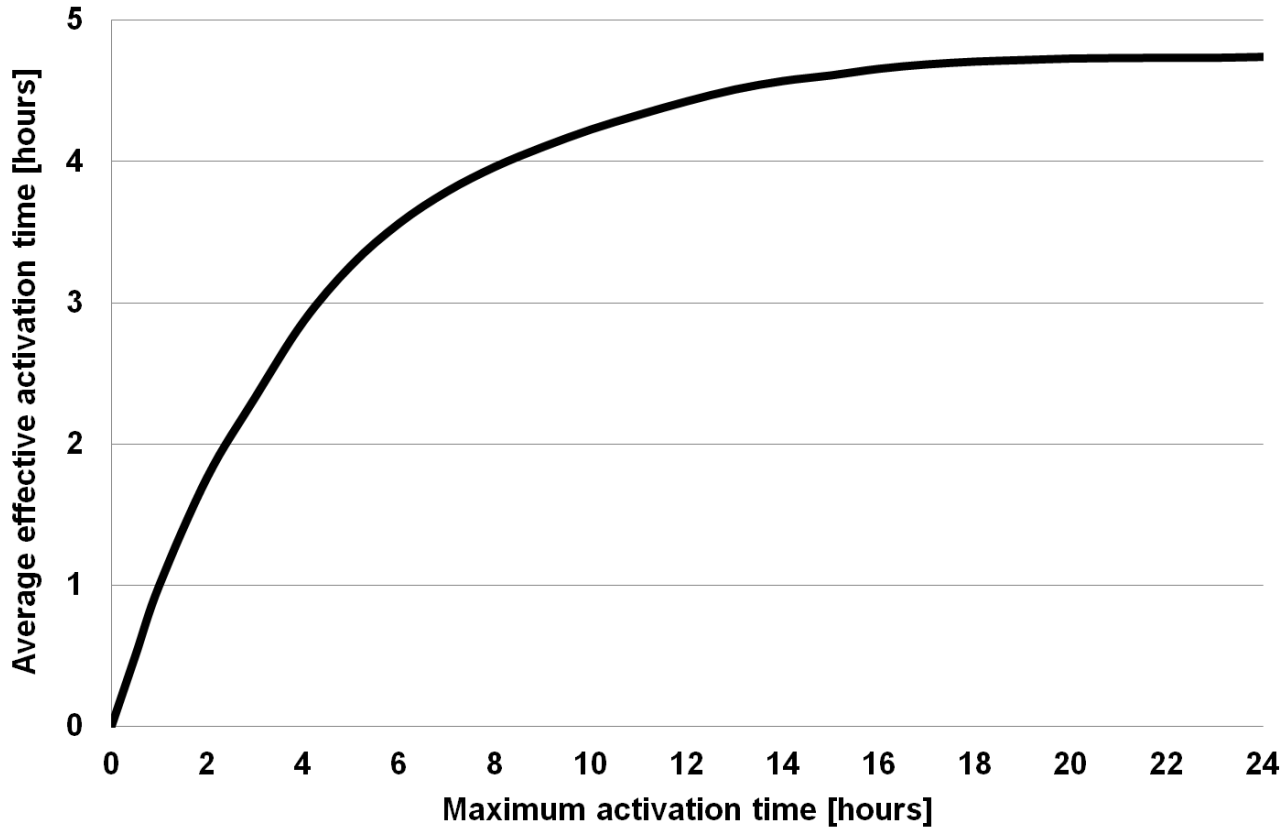

Fig. 7. *Average effective activation time as function of maximum activation time allowed for the heat storage control strategy.*

5.3. Impact of the building parameters on the energy flexibility

For the rest of this study, the maximum activation time of the heat accumulation strategy is kept at 24 hours. The building energy flexibility index has been calculated for 144 different study cases: two categories of building envelope performance, three classes of structural thermal inertia with three different sub-variations, two types of heating system and four additional indoor thermal mass configurations (empty room, furniture/indoor content, PCM furniture, PCM wallboards). The building cases with no heat accumulation strategy are taken as references for the index calculation. The results are shown on the **Fig. 8** where one can see the evolution of the energy flexibility index as function of building total effective thermal inertia (including structural thermal mass from the envelope and additional indoor thermal mass, if any).

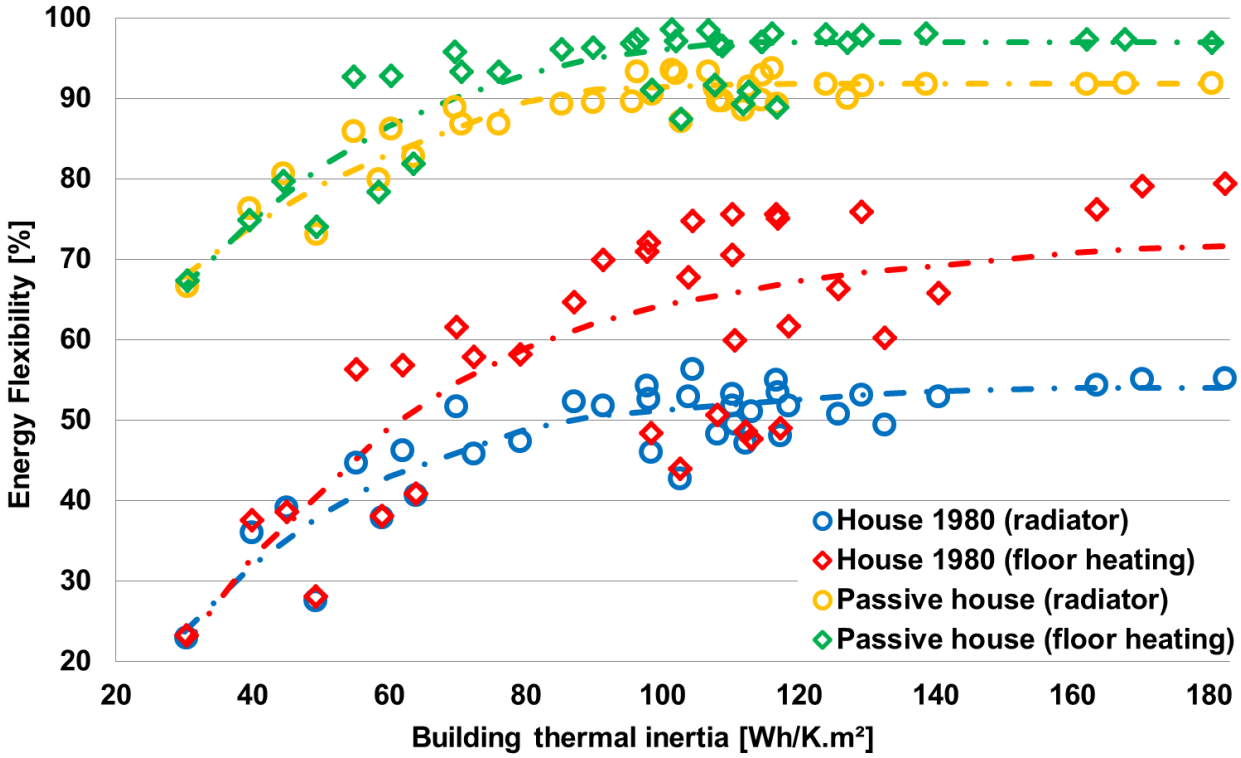

Fig. 8. *Evolution of the building energy flexibility as function of the thermal inertia.*

It is clear that low-insulation houses present a significantly lower energy flexibility index than high-insulation ones. Well-insulated dwellings have lower heating needs and can therefore shift it with a smaller storage capacity. Moreover, the efficiency of their envelope allows retrieval of a greater share of the accumulated thermal energy. However, one should keep in mind that low-insulation buildings can have a larger individual impact on the energy grid because the absolute amount of energy they are able to shift in time is about 4 times more important than high-insulation buildings.

Furthermore, the results show that all kinds of thermal mass, regardless of their nature or location in the house, can contribute to increase the overall building heat storage capacity and consequently its energy flexibility index. However, one can observe a group of outliers (clearly below the trend line) for houses with thermal inertia around 110 Wh/K.m² and equipped with under-floor heating system. These building cases are light-weight structure houses with under-floor heating system embedded in a wooden slab and with additional thermal mass from PCM wallboards or PCM furniture. The additional thermal mass brought by the PCM raises the effective thermal inertia of these houses to the one of heavy structure houses with concrete screed floors. However, when employing under-floor heating, the PCM thermal mass is not as activated as the one of a concrete screed floor and consequently does not improve the energy flexibility index with the same importance.

The positive impact on energy flexibility of increasing building thermal inertia stagnates for values above 80 Wh/K.m², especially for low energy buildings. Indeed, medium and heavy structure passive houses reach the maximum energy flexibility potential: there is no remaining heating energy use to be shifted in time and therefore increasing thermal inertia further for additional heat storage capacity is ineffective. In the case of medium and heavy structure low-insulation dwellings, additional thermal mass cannot compensate for the poor envelope performance which greatly limits the recovery of accumulated thermal energy and therefore the total energy flexibility potential.

Concerning heat emitters, the under floor heating system shows greater performance compared to convective radiators for medium and heavy structure buildings. The concrete screed where the under floor hydronic circuit is laid is highly activated, which allows a larger heat storage capacity. Moreover, radiant UFH system can provide the same level of thermal comfort with a lower indoor air temperature. This leads to a decrease of the ventilation and infiltration

thermal losses and therefore improves the heat accumulation efficiency and the building energy flexibility. The employment of UFH can thus increase the building energy flexibility by up to 44% and 8% for low-insulation and high-insulation dwellings respectively. In the case of light structure house, the under floor heating was integrated in a wooden floor which does not have a significant heat capacity. Consequently, the flexibility potential of low thermal mass buildings is not improved by the use of UFH.

5.4. Impact of additional indoor thermal mass on the building energy flexibility

This numerical study also focused on assessing the influence of three different types of additional indoor thermal mass element on the building energy flexibility. The comparison results are presented on **Fig. 9**. The energy flexibility and the thermal inertia of the reference empty buildings are stated in the table below the figure. The relative values of the flexibility improvement are indicated as percentage and the absolute values of the flexibility change are in between parentheses. One can see that PCM wallboards and furniture with integrated PCM can appreciably increase the energy flexibility potential of dwellings with low insulation and low structural thermal inertia. However, the improvement is reduced for well-insulated houses and very limited for buildings with medium and heavy structures.

In addition, it should be noted that PCMs and consequently PCM wallboards have a relatively low thermal conductivity. When positioned on the inner surface of construction elements in the thermal zone, the PCM wallboards obstruct the activation of the thermal mass underneath them. This is a problem in the case of buildings with heavy structures such as concrete or brick walls. The large heat storage capacity of these construction elements is nullified by the presence of the PCM wallboards and is barely compensated by the latter.

Concerning furniture and indoor content, they only account for a small share of the total effective thermal inertia of medium and heavy structure houses. It is thus not surprising that their impact on the building energy flexibility is almost negligible. Nevertheless, in the case of light structure dwellings, the influence of the indoor items is significant and should therefore be taken into account.

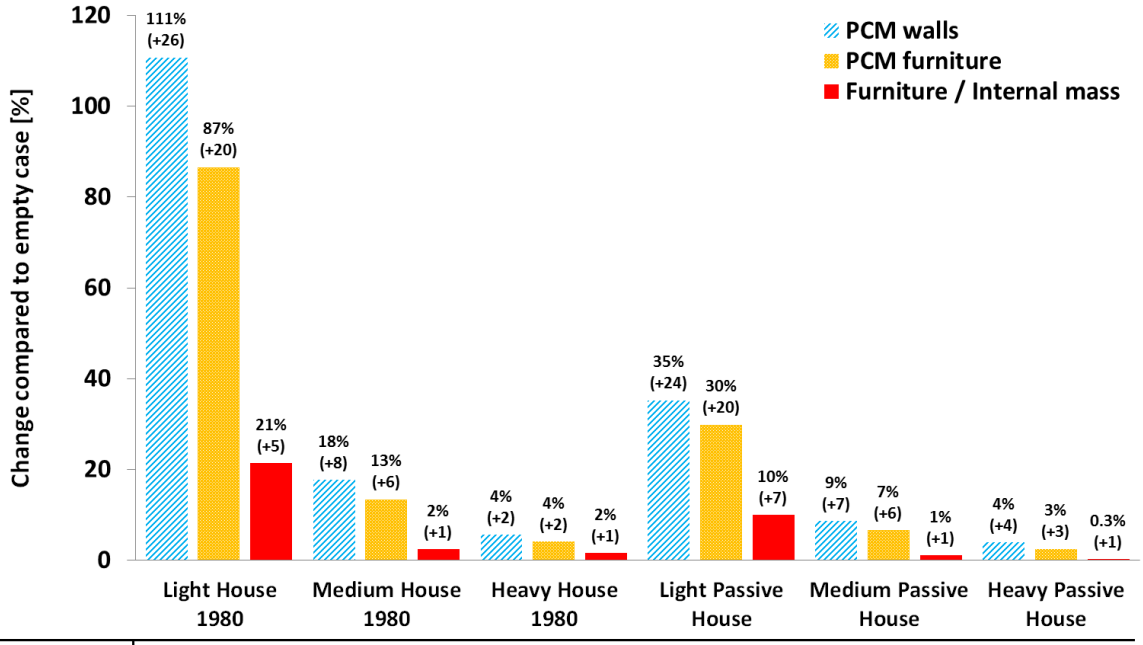

	Light House 1980	Medium House 1980	Heavy House 1980	Light Passive House	Medium Passive House	Heavy Passive House
Empty building energy flexibility [%]	23	45	53	67	86	90
Empty building thermal inertia [Wh/K.m²]	30	50	100	30	50	100

Fig. 9. *Change of building energy flexibility with additional internal thermal mass (radiator heating system and maximum activation time of 24 hours).*

5.5. Parametric sensitivity analysis

A statistical analysis of the results from the 144 different study cases presented in the previous sections is performed to rank the different building parameters by order of significance regarding the energy flexibility. The effect level of the parameters is assessed by the means of consecutive ANOVA (analysis of variance) tests on linear regression models with iterative deletion of the least significant term [56]. The results are presented in **Table 4** with the most significant building parameter regarding energy flexibility (highest F-value) on the top. From this statistical analysis, it can be concluded that the insulation level of the house has the main role in the building energy flexibility compared to the building total thermal inertia, type of heat emitter or the kind of additional indoor thermal mass.

Significance ranking	Building parameter	F-value
1	Envelope insulation level	685.4
2	Thermal inertia	91.4
3	Heating system type	42.3
4	Additional indoor thermal mass type	14.6

Table 4: *Significance ranking of the building parameters regarding energy flexibility*.

Secondly, a sensitivity analysis of the influence of the additional indoor thermal mass parameters regarding the light-structure dwellings energy flexibility is conducted. The flexibility factor is calculated for realistic low and high additional indoor thermal mass characteristic variations (see **Table 5**). Relative changes of the flexibility factor from the reference cases are indicated in the colored boxes (red color for positive variations and blue color for negative variations). A similar ANOVA statistical analysis is then performed on these results. The **Table 6** sums up the significance ranking of the different parameters of the three types of additional indoor thermal mass element. One can see that for indoor items/furniture elements, the surface heat transfer coefficient, the mass and the surface area of the elements play the main role while material density and thermal conductivity have little significance. For PCM furniture, the exposed surface area, the heat transfer coefficient and the PCM properties are the most significant parameters. For PCM wallboards, the characteristics of the phase change material layer have the dominant effects.

Indoor items / furniture	Parameter variation			Variation of building energy flexbility			
				House 80's		Passive House	
	Low	Reference	High	Low	High	Low	High
Surface heat transfer coefficient [W/K.m²]	5	7.7	10	-8.4%	18.4%	-5.1%	10.1%
Mass [kg/m² floor area]	20	60	100	-11.6%	10.6%	-6.0%	4.7%
Surface area [m²/m² floor area]	0.8	1.8	2.8	-8.8%	7.8%	-4.3%	3.1%
Material density [kg/m³]	150	715	1500	1.5%	-2.7%	0.5%	-1.0%
Material thermal conductivity [W/m.K]	0.1	0.3	0.5	2.3%	-0.5%	2.3%	-0.7%

PCM furniture parameters	Parameter variation			Variation of building energy flexbility			
				House 80's		Passive House	
	Low	Reference	High	Low	High	Low	High
Surface heat transfer coefficient [W/K.m²]	5	7.7	10	-7.0%	12.2%	-3.1%	3.2%
Furniture mass [kg/m² floor area]	20	60	100	-0.3%	2.6%	-0.2%	1.1%
PCM furniture surface area [m²/m² floor area]	0.8	1.8	2.8	-16.5%	9.3%	-10.6%	4.5%
Furniture material density [kg/m³]	150	715	1500	-0.4%	0.9%	-0.2%	0.5%
Furniture material thermal conductivity [W/m.K]	0.1	0.3	0.5	-0.4%	0.3%	-1.0%	0.5%
PCM layer thickness [cm]	0.5	1.5	3	-13.7%	4.2%	-5.1%	1.2%
PCM average thermal conductivity [W/m.K]	0.1	0.2	0.4	-11.4%	10.6%	-2.3%	1.3%
PCM latent heat of fusion [kJ/kg]	60	120	180	-19.4%	11.3%	-6.5%	1.2%

PCM Wallboard parameters	Parameter variation			Variation of building energy flexbility			
				House 80's		Passive House	
	Low	Reference	High	Low	High	Low	High
Surface heat transfer coefficient [W/K.m²]	5	7.7	10	-3.1%	1.3%	-1.2%	0.7%
PCM layer thickness [cm]	0.5	1.5	3	-15.7%	7.8%	-5.4%	1.2%
PCM average thermal conductivity [W/m.K]	0.1	0.2	0.4	-16.1%	8.0%	-5.3%	0.9%
PCM latent heat of fusion [kJ/kg]	60	120	200	-24.1%	9.8%	-8.5%	2.4%

Table 5: *Sensitivity analysis of the additional indoor thermal mass parameters.*

Indoor items/furniture

Significance ranking	Parameter	F-value
1	Surface heat transfer coefficient	30.1
2	Mass	18.3
3	Surface area	18.0
4	Material density	1.7
5	Material thermal conductivity	1.2

PCM furniture

Significance ranking	Parameter	F-value
1	Surface area	45.1
2	PCM latent heat of fusion	27.9
3	Surface heat transfer coefficient	13.8
4	PCM thermal conductivity	11.8

5	PCM layer thickness	10.9
6	Furniture mass	0.5
7	Furniture material density	0.1
8	Furniture material thermal conductivity	0.1

PCM wallboard

Significance ranking	Parameter	F-value
1	PCM latent heat of fusion	29.0
2	PCM layer thickness	12.6
3	PCM thermal conductivity	12.1
4	Surface heat transfer coefficient	0.5

Table 6: *Significance ranking of the additional thermal mass parameters regarding energy flexibility.*

6. Conclusion

The numerical study presented in this article has investigated the role of different building parameters in the space heating energy flexibility potential of a Danish single family house with a heat storage strategy based on indoor temperature set point modulation according to a price signal. The building energy flexibility index defined in this paper represents the capacity of the dwelling to shift its heating use in time by accumulating thermal energy in the indoor environment during low electricity price periods, and reducing its heating use during high electricity price periods.

The maximum thermal energy storage capacity of a building is mainly determined by its total effective thermal inertia. However, it was found that the envelope insulation level is the most important building parameter with respect to the capacity of a dwelling to shift its heating use in time. From the energy flexibility perspective, it is therefore more interesting to lower the building energy consumption and improve its storage efficiency rather than increasing the thermal inertia or changing the type of heating system. Nevertheless, it should be noted that poorly insulated houses, despite their limited energy flexibility index, can have a larger individual impact on the energy grid because the absolute amount of energy they can shift in time is more important than the one of highly insulated houses. Low-energy houses also have a higher risk of overheating when performing thermal storage in the indoor space. Moreover, passive houses have very low space heating needs with a shorter heating season. Consequently, their space heating energy flexibility is only available during the coldest days of the year but not during transition seasons, unlike poorly insulated houses.

In order to increase the effective thermal inertia of lightweight structure dwellings and consequently improve their energy flexibility, the integration of phase change materials in inner surface wallboards or in furniture elements seems to be a good solution. In the current numerical study, the PCM wallboards could increase the energy flexibility index by up to 111% and 35% in the cases of low-insulation and high-insulation light-structure houses respectively. Similarly, furniture with integrated PCM could increase the energy flexibility index by up to 87% and 30% in the cases of low-insulation and high-insulation light-structure houses respectively. It should be pointed that PCM wallboards should not be placed on heavy construction elements. They screen the thermal activation of the material layers placed behind them and barely provide the same heat storage capacity as traditional concrete or brick walls. In the case of medium and heavy structure houses, additional thermal inertia only marginally improves the energy flexibility potential. In addition, the use of UFH system instead of convective radiators can activate more of the building structural thermal mass with a reduced indoor air temperature. It can thus lead to a building energy flexibility improvement of up to 44% and 8% for low-insulation and high-insulation dwellings respectively.

This paper also demonstrated that the empty space assumption for dynamic energy simulations was not appropriate for lightweight structure buildings with less than 50 Wh/K.m² of thermal inertia. Transient thermal behaviour and total heat storage capacity can be significantly influenced by the presence of items and furniture in the indoor environment. It

was found that the assessment of the time constant of such building can be increased by up to 43% and the energy flexibility index by up to 21% when indoor items are taken into account.

Other researchers have drawn similar conclusions regarding space heating energy flexibility but using different flexibility indexes. This reinforces the robustness of the current study's results. However, further work is needed in these promising research topics of demand side management and building energy flexibility strategy. Novel methodologies should be developed and tested for assessing building's ability to respond to the grids' need. More studies should also be made on the acceptability of users regarding domestic heat storage strategies with external control signals. Concerning numerical simulations, knowledge has to be gained about the interaction between the indoor content elements, such as furniture, and the indoor environment for a better prediction of the dynamic building thermal behaviour. Finally, the potential for phase change materials integrated in furnishing elements should be investigated further. The design of these latent heat thermal energy storage systems should be optimized in accordance to a certain heat accumulation strategy and precise boundary conditions.

Acknowledgements

This work was financed by the ENOVHEAT project which is funded by Innovation Fund Denmark (contract no 12-132673) and was carried out partly within the framework of IEA EBC Annex 67 Energy Flexible Buildings.

References

[1] W.M. Beurskens, M. Hekkenberg, P. Vethman. Renewable energy projections as published in the national energy action plans of the European member states. Report no. ECN-E-10-069. ECN and European Environment Agency. https://www.ecn.nl/docs/library/report/2010/e10069.pdf. February 2011 (Accessed 17 October 2017).

[2] Energy Strategy 2050 − from coil, oil and gas to green energy. The Danish Government. http://www.kebmin.dk/sites/kebmin.dk/files/news/from-coaloil-and-gas-to-green-energy/Energy%20Strategy%202050%20web.pdf. February 2011 (Accessed 17 October 2017).

[3] B.V. Mathiesen, H. Lund, D. Connolly, H. Wenzel, P.A. Østergaard, B. Möller, S. Nielsen, I. Ridjan, P. Karnøe, K. Sperling, F.K. Hvelplund. Smart Energy Systems for coherent 100% renewable energy and transport solutions. Applied Energy 145 (2015) 139–154.

[4] Building Performance Institute Europe (BPIE), Europe's Buildings under the Microscope, Executive Summary 2011. http://bpie.eu/wp-content/uploads/2015/10/HR_EU_B_under_microscope_study.pdf. 2011 (Accessed 17 October 2017).

[5] K. Hedegaard, B.V. Mathiesen, H. Lund, P. Heiselberg. Wind power integration using individual heat pumps – Analysis of different heat storage options. Energy 47 (2012) 284–93.

[6] G. Reynders, J. Diriken, D. Saelens. A generic quantification method for the active demand response potential of structural storage in buildings, 14th IBPSA conference, Building Simulation 2015, Hyderabad, India (2015).

[7] B. Favre, B. Peuportier. Application of dynamic programming to study load shifting in buildings. Energy and Buildings 82 (2014) 57-64.

[8] G. Masy, E. Georges, C. Verhelst, V. Lemort, P. André. Smart grid energy flexible buildings through the use of heat pumps and building thermal mass as energy storage in the Belgian context. Science and Technology for the Built Environment 21 (2015) 800-811.

[9] J. Le Dréau, P. Heiselberg. Energy flexibility of residential buildings using short term heat storage in the thermal mass. Energy 111 (2016) 991-1002.

[10] G. Reynders, T. Nuytten, D. Saelens. Potential of structural thermal mass for demand-side management in dwellings. Building and Environment 64 (2013) 187-199.

[11] A. Arteconi, D. Costola, P. Hoes, J.L.M. Hensen. Analysis of control strategies for thermally activated building systems under demand side management mechanisms. Energy and Buildings 80 (2014) 384-393.

[12] R. Barzin, J.J.J. Chen, B.R. Young, M.M. Farid. Applpication of PCM underfloor heating in combination with PCM wallboards for space heating using price based control system. Applied Energy 148 (2015) 39-48.

[13] A. Bastani, F. Haghighat, C.J. Manzano. Investigating the effect of control strategy on the shift of energy consumption in a building integrated with PCM wallboard. In: 6th International Building Physics Conference, IBPC (2015).

[14] H. Johra and P. Heiselberg. Influence of internal thermal mass on the indoor thermal dynamics and integration of phase change materials in furniture for building energy storage: A review. Renewable and Sustainable Energy Reviews 69 (2017) 19-32.

[15] Energistyrelsen, Danmarks Energifremskrivning 2012 . https://ens.dk/sites/ens.dk/files/Basisfremskrivning/danmarks_energifremskrivning_2012_endelig_v1.2.pdf. October 2012 (Accessed 17 October 2017).

[16] J. Krag, K.B. Wittchen. Development of two Danish building typologies for residential buildings. Energy and Buildings 68 Part A (2014) 79-86.

[17] R.A. Lopes, A. Chambel, J. Neves, D. Aelenei, J. Martins. A literature review of methodologies used to assess the energy flexibility of buildings. Energy Procedia 91 (2016) 1053-1058.

[18] G. Reynders, R.A. Lopes, A. Marszal-Pomianowska, D. Aelenei, J. Martins, D. Saelens. Energy flexible buildings: An evaluation of definitions and quantification methodologies applied to thermal storage. Energy and Buildings 166 (2018) 373-390.

[19] http://www.iea-ebc.org/projects/ongoing-projects/ebc-annex-67/ (Accessed 17 October 2017).

[20] S.J. Østergaard, A. Marszal-Pomianowska, R. Lollini, W. Pasut, A. Knotzer, P. Engelmann, A. Stafford, G. Reynders. IEA EBC Annex 67 Energy Flexible Buildings. Energy and Buildings 155 (2017) 25-34.

[21] J. Le Dréau. Demand-side management of heating need in residential buildings, CLIMA 2016 – proceedings of the 12th REHVA world congress.

[22] ISO 13786:2007, Thermal performance of building components – Dynamic thermal characteristics – Calculation methods.

[23] D. Maillet, S. André, J.-C. Batsale, A. Degiovanni, C. Moyne. Thermal Quadrupoles, Wiley, New York (2000).

[24] F. Kuznik, J. Virgone, J. Noel. Optimization of a phase change material wallboard for building use. Applied Thermal Engineering 28 (2008) 1291–8.

[25] ISO 6946:2007, Building components and building elements – thermal resistance and thermal transmittance – calculation method.

[26] T.S. Larsen, C. Brunsgaard. Komfort Husene: erfaringer, viden og inspiration. Saint-Gobain Isover a/s (2010).

[27] ISO 13790:2008, Energy performance of buildings – Calculation of energy use for space heating and cooling.

[28] French Building Energy and Thermal Regulation 2012, CSTB FR (2012)

[29] K. Ovesen. SBi Anvisning 175-Varmeanlæg med vand som medium. Danish Building Research Institute - SBi (2000).

[30] EN 1264, Water based surface embedded heating and cooling systems.

[31] EN 15377, Heating systems in buildings – Design of embedded water based surface heating and cooling system.

[32] ISO 11855, Building environment design – Design, dimensioning, installation and control of embedded radiant heating and cooling systems.

[33] Uponor, Heating and cooling solutions - technical guidelines. https://www.uponor.co.in/~/media/countryspecific/international/download-centre/indoor_climate/underfloor-heating/brochures/technical-guidelines-home-comfort.pdf?version=1. March 2009 (Accessed 17 October 2017).

[34] Uponor, Installation guide for underfloor heating systems - technical information (2016).

[35] P.G. Wang, M. Scharling, K.P. Nielsen, K.B. Wittchen, C. Kern-Hansen. DMI Technical Report 13-19: 2001-2010 Danish Design Reference Year - Reference Climate Dataset for Technical Dimensioning in Building, Construction and other Sectors (2013).

[36] R.L. Jensen, J. Nørgaard, O. Daniels, R.O. Justesen. Person og forbrugsprofiler: bygningsintegreret energiforsyning. Aalborg University, DCE Technical Reports No. 69 (2011).

[37] H. Johra, P. Heiselberg. Description and validation of a MATLAB - Simulink single family house energy model with furniture and phase change materials (Update). Aalborg University, DCE Technical Reports No. 238 (2018). http://vbn.aau.dk/files/270078674/Description_and_Validation_of_a_MATLAB_Simulink_Single_Family_House_Energy_Model_with_Furniture_and_Phase_Change_Materials_Update_.pdf (Accessed 11 April 2018).

[38] C.R.H. Bahl. EnovHeat project summary: development of efficient novel magnetocaloric heat pumps. http://www.enovheat.dk/Research/ProjectSummary. 2015 (Accessed 17 October 2017).
[39] A.S. Kalagasidis, C. Rode, M. Woloszyn. HAM-Tools – a whole building simulation tool in Annex 41. Proceedings of the IEA ECBCS Annex 41 Closing Seminar (2008).
[40] G. Reynders, J. Diriken, D. Saelens. Quality of grey-box models and identified parameters as function of the accuracy of input and observation signals. Energy and Buildings 82 (2014) 263-274.
[41] BSim software - User's Guide – tsbi5. Danish Building Research Institute - SBi (2013).
[42] S. Adams, M. Holmes. Determining time constants for heating and cooling coils. Building Services Research & Information Association, UK (1977).
[43] University of Wisconsin-Madison Solar Energy Laboratory, TRANSSOLAR Energietechnik GmbH, CSTB, TESS. Type 31: Pipe or duct model. TRNSYS 17 – Mathematical Reference 2012, 186 – 188.
[44] M. Scarpa, K. Grau, B.W. Olesen. Development and validation of a versatile method for the calculation of heat transfer in water-based radiant systems. Eleventh International IBPSA Conference, Glasgow, Scotland, 27-30 (July 2009).
[45] R. Prapainop, K. Maneeratana. Simulation of ice formation by the finite volume method. Songklanakarin J. Sci. Technol. 26 (2004) 55-70.
[46] P. Verma, Varun, S.K. Singal, Review of mathematical modeling on latent heat thermal energy storage systems using phase-change material. Renewable and Sustainable Energy Reviews 12 (2008) 999-1031.
[47] DuPont Energain®, Technical Datasheet. http://www.cse.fraunhofer.org/hs-fs/hub/55819/file-14736951-pdf/docs/energain_flyer.pdf. 2012 (Accessed 17 October 2017).
[48] H. Johra, P. Heiselberg, J. Le Dréau. Numerical analysis of the impact of thermal inertia from the furniture / indoor content and phase change materials on the building energy flexibility. Proceedings of the 15th IBPSA Conference, International Building Performance Simulation Association, San Francisco, CA, USA. Aug. 7-9 (2017).
[49] P. Raftery, E. Lee, T. Webster, T. Hoyt, F. Bauman. Effect of furniture and contents on peak cooling load. Energy and Buildings 85 (2014) 445-457.
[50] H. Johra, K. Filonenko, P. Heiselberg, C. Veje, T. Lei, S. Dall'Olio, K. Engelbrecht, C. Bahl. Integration of a magnetocaloric heat pump in a low-energy residential building. Building Simulation: An International Journal (2018).
[51] T.Q. Péan, J. Salom, J. Ortiz. Potential and optimization of a price-based control strategy for improving energy flexibility in Mediterranean buildings. In: CISBAT 2017 International Conference – Future Buildings & Districts – Energy Efficiency from Nano to Urban Scale, 6-8 September 2017, Lausanne, Switzerland.
[52] EnergiNet.dk. Market data (elspot price in Western Denmark). www.energinet.dk/en/el/engrosmarked/udtraek-af-markedsdata/Sider/default.aspx. 2009 (Accessed 17 October 2017).
[53] EN ISO 7730. Ergonomics of the thermal environment-analytical determination of thermal comfort by using calculation of the PMV and PPD indices and local thermal comfort criteria (2005).
[54] ASHRAE Standard, Standard 55 – 2004. Thermal environmental conditions for human occupancy.
[55] J.P. Holman. Experimental methods for engineers (Sixth edition). USA: McGraw-Hill, Inc (1994).
[56] D.C. Montgomery. Design and Analysis of Experiments, Eighth edition. John Wiley & Sons Incorporated (2012).